AIP Journal of Applied Physics

Optical third-order nonlinearity by nanosecond and picosecond pulses in Cu nanoparticles in ion-implanted silica

C. Torres-Torres, J. A. Reyes-Esqueda, J. C. Cheang-Wong, A. Crespo-Sosa, L. Rodríguez-Fernández, and A. Oliver

Citation: Journal of Applied Physics **104**, 014306 (2008); doi: 10.1063/1.2952040
View online: http://dx.doi.org/10.1063/1.2952040
View Table of Contents: http://scitation.aip.org/content/aip/journal/jap/104/1?ver=pdfcov
Published by the AIP Publishing

Optical third-order nonlinearity by nanosecond and picosecond pulses in Cu nanoparticles in ion-implanted silica

C. Torres-Torres,[a] J. A. Reyes-Esqueda,[a] J. C. Cheang-Wong, A. Crespo-Sosa, L. Rodríguez-Fernández, and A. Oliver
Instituto de Física, Universidad Nacional Autónoma de México, A.P. 20-364, México Distrito Federal 01000, Mexico

(Received 12 March 2008; accepted 30 April 2008; published online 8 July 2008)

We report a study of the Kerr effect and nonlinear optical absorption in a high-purity silica sample containing Cu nanoparticles prepared by ion implantation. With a vectorial self-diffraction experiment, we measured the tensorial components of the third-order nonlinear optical susceptibility response at 532 nm with pulses of 7 ns and 26 ps. We identified thermal effect as the main mechanism responsible for the nonlinear refraction in the nanosecond regime and electronic polarization for the picosecond regime. We observed saturable optical absorption in both regimes studied. We also measured the ablation threshold for this material, finding that the contribution of the linear optical absorption to the ablation threshold in each case can be different due to the presence of hot electrons. © *2008 American Institute of Physics*. [DOI: 10.1063/1.2952040]

I. INTRODUCTION

The study of the optical properties of different metallic nanostructures such as nanocomposites,[1] nanorods,[2] or nanoparticles[3] (NPs) has been extensively investigated in the past years in order to improve their response. One of the most attractive characteristics of nanometer-sized particles prepared by ion implantation is that they exhibit very good stability[4] and offer the possibility of potential applications such as waveguides or other optical components associated with nonlinear optical effects.[5] Particularly, the third-order nonlinear optical response, described by the $\chi^{(3)}$ susceptibility, is responsible for effects such as third harmonic generation, self-focusing, Raman scattering, Brillouin scattering, and phase conjugation, among others.[6] Applications of these optical effects are innumerable. In the majority of the optical materials, the refractive index (RI) can be expressed as $n=n_0+n_2I$, where n_0 represents the linear RI in weak field, this being the case in which n is practically equal to n_0; I is the light intensity in the medium and n_2 is the nonlinear RI. In a similar way, the intensity dependent absorption coefficient is defined as $\alpha(I)=\alpha_0+\beta I$, where α_0 and β represent the linear and nonlinear absorption coefficients, respectively. It is well known that the real part of $\chi^{(3)}$ is related to the optical Kerr effect, i.e., proportional to n_2, and the imaginary part of $\chi^{(3)}$ is related to the nonlinear absorption, i.e., proportional to β. While a positive β means the occurrence of two photon absorption, in the case of a negative β, the actual effect is saturable absorption. Several methods have been developed to measure the refractive and absorptive contributions to the nonlinearity, mainly related to z-scan[7] and four-wave mixing techniques.[8] Recently, a method based on vectorial self-diffraction measurements has been introduced for measuring the nonlinear RI n_2 and the nonlinear absorption coefficient β, with the advantage of identifying at the same time the mechanism responsible for the nonlinearity.[9]

In this work, we used this method for measuring the optical Kerr effect and nonlinear absorption at 532 nm with pulses of 7 ns and 26 ps in a high-purity silica sample implanted with Cu ions. We obtained significant intensities of nonlinearity and deduced the physical mechanisms responsible for the absorptive and refractive nonlinearities in such a nanocomposite. Since the nonlinear response can be related to particular components of $\chi^{(3)}$ for different physical mechanisms of nonlinearity of index, when measuring it in isotropic media, it is possible to identify all the components of $\chi^{(3)}$ by comparing the vectorial self-diffracted effect for different temporal regimes. We also show the results obtained for laser ablation in the material due to single nanosecond and picosecond pulses, exhibiting the importance of hot electrons in both regimes.

II. EXPERIMENTAL DETAILS

For the preparation of the NPs, high-purity silica glass plates ($16\times16\times1$ mm^3) with OH content less than 1 ppm and an impurity content less than 20 ppm were implanted at room temperature with 2 MeV Cu^{2+} ions at a fluence around $(4.0\pm0.3)\times10^{16}$ ions/cm^2. After implantation, the samples were cut into identical small pieces (35 mm^2) and thermally annealed in a reducing atmosphere of $50\%H_2+50\%N_2$ at a temperature of 900 °C for 1 h.[10] The metal distribution and fluences were determined by Rutherford backscattering spectrometry (RBS) measurements using a 4 MeV $^4He^+$ beam. Ion implantation and RBS analysis were performed using the IFUNAM 3 MV tandem accelerator NEC 9SDH-2 Pelletron.

For the self-diffraction experiments, we used two different frequency doubled neodymium doped yttrium aluminum garnet lasers with a $\lambda=532$ nm wavelength and pulse durations of 7 ns and 26 ps full width at half maximum, respectively. In both cases the beams had linear polarization. The

[a]Authors to whom correspondence should be addressed. Electronic addresses: crstorres@yahoo.com.mx and reyes@fisica.unam.mx.

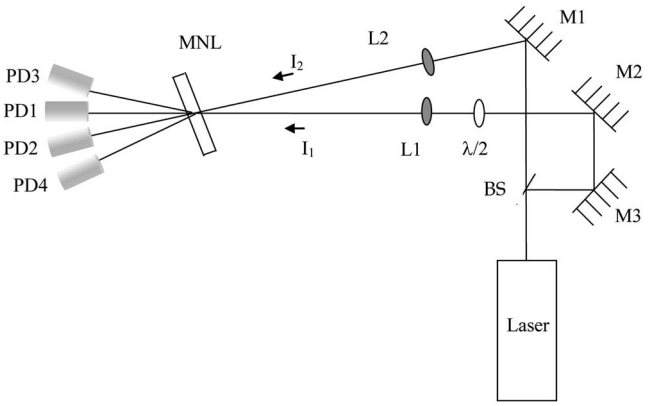

FIG. 1. Experimental setup used for self-diffraction measurements.

maximum pulse energy in the experiments was 6 mJ for the 7 ns pulses and 1 mJ for the 26 ps pulses. The intensity rate $I_1:I_2$ was 1:2. The radius of the beam waist at the focus in the sample was measured to be 0.15 mm for the nanosecond experiments and 1.1 mm for the picosecond ones. Figure 1 shows the experimental setup, where L1 and L2 represent the focusing system of lenses, BS is a beam splitter, M1–M3 are mirrors, S is the sample, and PD1–PD4 are photodetectors with integrated filters.

To measure the ablation threshold fluence in the nanocomposite, we removed the BS in the experimental setup and oriented the sample for normal incidence of the laser. The spot area was kept constant while the beam energy was increased until finding the ablation fluence. This particular experiment was determined by monitoring the linear absorption of the sample after each single laser pulse until significant changes in the spectrum were observed, which could also be perceived with the naked eye.

III. RESULTS AND DISCUSSION

Figure 2 shows the linear optical absorption of the nanocomposite, where the surface plasmon resonance band around 560 nm, associated with the spherical-like shaped Cu NPs of 4–6 nm in diameter embedded into the silica sample, is clearly observed.[11]

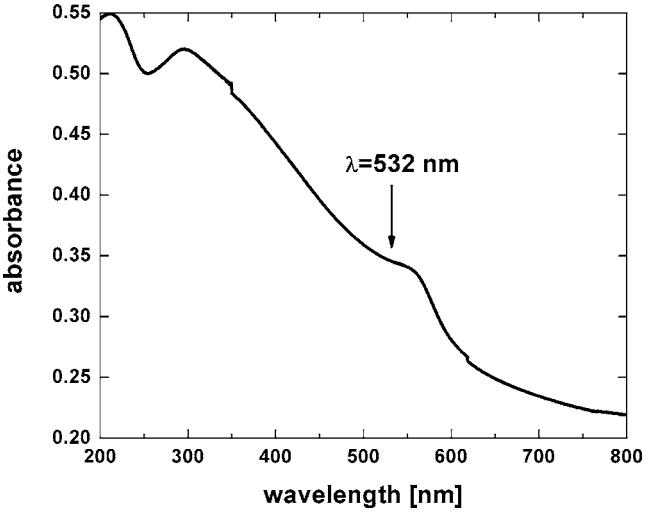

FIG. 2. Absorbance of the silica sample containing Cu NPs. The λ =532 nm laser wavelength is indicated.

For the nonlinear optical response, according to our previous studies,[9] we used Eqs. (1)–(4) to describe the interaction of the incident and the self-diffracted waves in the nonlinear absorbing media:

$$E_{1\pm}(z) = [J_0(\Psi_{\pm}^{(1)})E_{1\pm}^0 + iJ_1(\Psi_{\pm}^{(1)})E_{2\pm}^0] \times \exp\left(-i\Psi_{\pm}^{(0)} - \frac{\alpha(I)z}{2}\right), \quad (1)$$

$$E_{2\pm}(z) = [J_0(\Psi_{\pm}^{(1)})E_{2\pm}^0 - iJ_1(\Psi_{\pm}^{(1)})E_{1\pm}^0] \times \exp\left(-i\Psi_{\pm}^{(0)} - \frac{\alpha(I)z}{2}\right), \quad (2)$$

$$E_{3\pm}(z) = [iJ_1(\Psi_{\pm}^{(1)})E_{1\pm}^0 - J_2(\Psi_{\pm}^{(1)})E_{2\pm}^0] \times \exp\left(-i\Psi_{\pm}^{(0)} - \frac{\alpha(I)z}{2}\right), \quad (3)$$

$$E_{4\pm}(z) = [-iJ_1(\Psi_{\pm}^{(1)})E_{2\pm}^0 - J_2(\Psi_{\pm}^{(1)})E_{1\pm}^0] \times \exp\left(-i\Psi_{\pm}^{(0)} - \frac{\alpha(I)z}{2}\right), \quad (4)$$

where $E_{1\pm}(z)$ and $E_{2\pm}(z)$ are the complex amplitudes of the circular components of the transmitted wave beams; $E_{3\pm}(z)$ and $E_{4\pm}(z)$ are the amplitudes of the self-diffracted waves, while $E_{1\pm}^0$ and $E_{2\pm}^0$ are the amplitudes of the incident waves; $a(I)$ is the intensity dependent absorption coefficient, I is the total irradiance of the incident beams, $J_m(\Psi_{\pm}^{(1)})$ stands for the Bessel function of order m, z is the thickness of the nonlinear media, and

$$\Psi_{\pm}^{(0)} = \frac{4\pi^2 z}{n_0\lambda}[A(|E_{1\pm}|^2 + |E_{2\pm}|^2) + (A+B)(|E_{1\mp}|^2 + |E_{2\mp}|^2)], \quad (5)$$

$$\Psi_{\pm}^{(1)} = \frac{4\pi^2 z}{n_0\lambda}[AE_{1\pm}E_{2\pm}^* + (A+B)E_{1\mp}E_{2\mp}^*], \quad (6)$$

are the phase increments. Here $A=6\chi_{1122}^{(3)}=3\chi_{1122}^{(3)}+3\chi_{1212}^{(3)}$ and $B=6\chi_{1221}^{(3)}$, where the components of the third-order susceptibility tensor $\chi^{(3)}$ for an isotropic material are related by[6]

$$\chi_{1111}^{(3)} = \chi_{1122}^{(3)} + \chi_{1212}^{(3)} + \chi_{1221}^{(3)}. \quad (7)$$

Given the isotropy of the material, the nonlinear RI n_2 and the nonlinear absorption coefficient β are usually related to $\chi^{(3)}$ (esu) by[7]

$$\chi^{(3)} = 2n_0^2\varepsilon_0 c n_2 + i\frac{n_0^2\varepsilon_0 c^2}{\omega}\beta, \quad (8)$$

where ε_0 represents the permittivity of the vacuum and ω the optical frequency. The magnitude of the third-order nonlinear optical susceptibility $\chi^{(3)}$ can be expressed as

$$|\chi^{(3)}| = \sqrt{(\mathrm{Re}\,\chi^{(3)})^2 + (\mathrm{Im}\,\chi^{(3)})^2}. \quad (9)$$

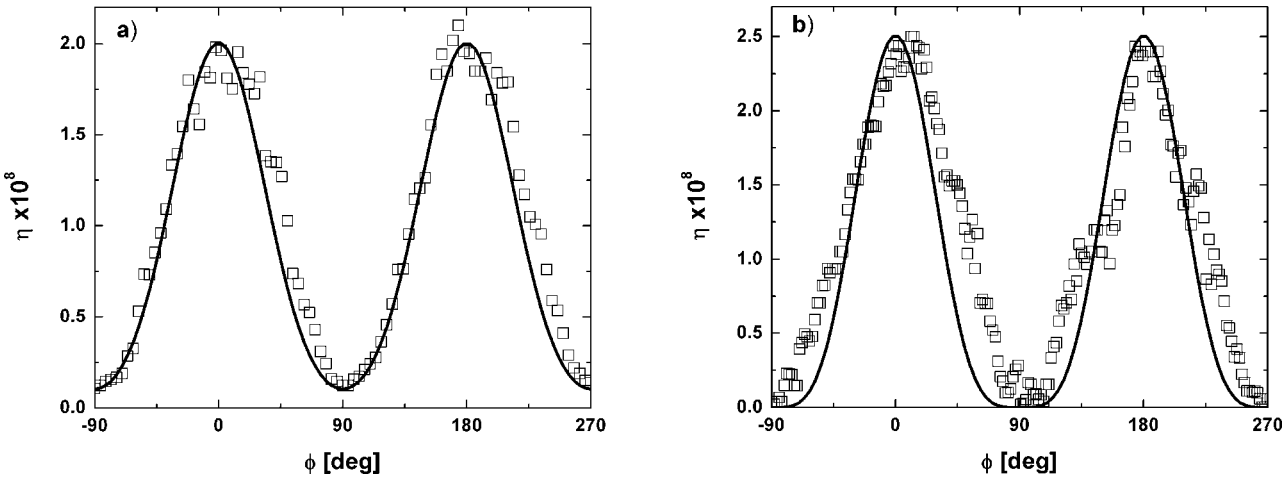

FIG. 3. Self-diffraction efficiency as a function of the angle ϕ between planes of polarization of the incident waves: (a) picosecond regime, (b) nanosecond regime.

Defining the self-diffraction efficiency η as the ratio between the intensities of the first and the zero order of diffraction of the incident beam, we can write

$$\eta = \frac{I_3}{I_1}. \tag{10}$$

In the nanosecond regime, the transmitted intensities measured by the four photodetectors were $I_1 = 179$ MW/cm^2, $I_1 = 360$ MW/cm^2, $I_1 = 439$ MW/cm^2, and $I_1 = 978$ MW/cm^2 for parallel polarizations. For the picosecond experiments, these intensities were $I_1 = 150$ MW/cm^2, $I_1 = 300$ MW/cm^2, $I_1 = 3$ MW/cm^2, and $I_1 = 6$ MW/cm^2, respectively. Figure 3 shows numerical and experimental self-diffraction efficiencies in the material for both temporal regimes.

For orthogonal incident polarizations in the sample, we did not observe any self-diffracted intensity in the nanosecond regime. By analyzing Eqs. (1)–(4), one can infer that this result is consistent with $B=0$ for the self-diffraction intensity response, implying also that $B/A=0$.[12] This relationship allows us to point out the physical mechanism behind the nonlinear optical response.[6,13] In particular, from Eqs. (5) and (6), it is possible to deduce that $B=0$ indicates that the induced birefringence is equivalent for orthogonal polarizations, and as a consequence, the physical mechanism responsible for the measured nonlinearity of index is isotropic. Because the nanosecond experiments were performed with a wavelength very close to resonance and the optical absorption is rather large, we can conclude that a thermal effect is the most likely reason for the observed nonlinear refraction.[12,13] As a consequence, $\chi^{(3)}_{1221}=0$ and the contribution to $\chi^{(3)}_{1111}$ comes only from $\chi^{(3)}_{1122}$ and $\chi^{(3)}_{1212}$, each having an identical value due to the isotropy of the material. On the contrary, for the picosecond regime, a nonzero self-diffraction effect for all the angles between planes of polarization can be observed from Fig. 3. By fitting the numerical and experimental data and using Eqs. (5) and (6), we obtained the relation between parameters A and B, resulting in $B/A=1$. This result allows us to identify the electronic polarization as the mechanism responsible for the observed nonlinear refraction in this temporal regime. As a result, the contribution to $\chi^{(3)}_{1111}$ comes from both A and B. However, they have the same value, which gives that $\chi^{(3)}_{1111}=3\chi^{(3)}_{1221}$ in this case.

By comparing numerical simulations of Eqs. (1)–(4) for the data obtained from the self-diffracted intensities in CS_2 and for those obtained from the Cu nanocomposite, first we found the value of β for the two temporal regimes, then $\chi^{(3)}_{1111}$, and finally n_2 in both cases, as it is shown in Table I. These magnitudes have an error bar of approximately $\pm 10\%$.

As it can be observed from the table, there is a stronger nonlinear response for the nanosecond regime in comparison with the picosecond one. In particular, the negative sign for β in both regimes indicates the presence of saturable optical absorption for the nanocomposite. Since we have performed the measurements very close to the Cu plasmon resonance, this result can be attributed to the participation of linear absorption in nonlinear processes, which enhances thermal effects, in particular. As it is explained in Ref. 14, when exciting a metal NP near its surface plasmon resonance, an important part of the incident energy is absorbed by its conduction electrons, whose specific heat is rather weak, increasing then their temperature by several hundred degrees. These so-called hot electrons are the main responsible for the saturation of the nanocomposite's optical absorption, which is a nonlinear process. By referring again to Ref. 14, it is important to stress the role of the local-field factor relating the microscopic (NP) and the macroscopic (nanocomposite) third-order susceptibilities. The square of this factor is nearly real negative and since the macroscopic observation is that the absorption of the macroscopic composite decreases, one

TABLE I. Nonlinear response and ablation threshold for the Cu nanocomposite in the nanosecond and picosecond regimes.

Pulse duration	n_2 (m^2/W)	β (m/W)	$\lvert\chi^{(3)}\rvert$ (esu)	Ablation threshold (J/cm^2)
7 ns	-1.15×10^{-15}	-2×10^{-10}	8.8×10^{-10}	8.41
26 ps	-1.1×10^{-16}	-2×10^{-13}	8.4×10^{-11}	2.14

arrives to the surprising result implying that, locally, the absorption of the Cu NPs at 532 nm increases due to the hot-electron contribution and to the negative sign of the local-field correction. Actually, what has been argued to happen is a transient redistribution of the equilibrium plasmon band due to a modification in the dielectric constant of the NP.[15–17] As a result, the absorption diminishes around the peak of the plasmon band while that at the wings is increased. As a consequence, according to our measurements, we would think that absorption at 560 nm decreases but that at 532 nm increases. In the nanosecond regime, this thermal effect is stronger and will produce more hot electrons, making the sample more transparent than that for the picosecond case, in agreement with the difference in β.

Comparing with the literature,[1,17–21] we observe a similar nonlinear response for similar systems. However, it is worth remarking that there is no clear trend that indicates whether the nanocomposite will show saturable or reverse saturable absorption. In other words, although the effect of hot electrons on the nonlinear optical properties of the nanocomposite seems well established from a physical point of view, the experimental measurements are an indication of something only partially understood. For instance, as it is discussed in Ref. 22, if a quantum well approach were used to analyze the optical response of the nanocomposite, the conduction electron intraband transitions would play a more important role in the origin of the optical nonlinearity than the hot electrons.[14] Therefore, our results, besides their own relevance for potential applications, just confirm the necessity of a deeper physical approaching into the optical response of metallic nanocomposites. In this direction, we intend to perform more experiments measuring self-diffraction efficiencies including anisotropic metallic nanocomposites,[23,24] which would allow to determine the separate components of the third-order susceptibility tensor and their physical contribution to the optical response.

With respect to the ablation measurements, for intensities of GW/cm^2, we observed that the ablation threshold was lower for the picosecond regime in comparison to the nanosecond one, being 2.14 and 8.41 J/cm^2, respectively, with an error bar of $\pm 5\%$. For the nanosecond case, considering the lack of data for materials at high temperatures and pressures, as well as the inhomogeneity of the laser beam, this ablation threshold is in agreement with the values previously found in heterogeneous systems.[25,26] In these cases, ablation of the entire irradiated zone would be a consequence of thermal stress provoked by the rapid energy absorption performed by the inclusions embedded into it. This entire zone, the NPs and the matrix layer containing them, reaches temperatures as high as the melting temperature, or even evaporation, of the NPs. The thermal stresses caused by this temperature increment can be above the tensile strength.

In the picosecond regime, the ablation threshold depended strongly on the spot area, decreasing when the area diminished too. Although it could be said that the experimental value for this case agrees qualitatively with an explanation based on thermal and deformation stresses as stated above, one must be aware that, in this case, the energy is absorbed mainly by the conduction electrons of the NPs, being as a consequence not immediately available as heat. The time required for hot electrons to transfer their absorbed energy to the lattice has been estimated to be about some picoseconds,[27] which is about the pulse duration. Additionally, the thermal evolution of these hot electrons is not well known and the spot area dependence is against a thermal stress explanation since a smaller spot would mean better lateral heat dissipation and, therefore a higher ablation threshold, this being not the case but the contrary. One possible mechanism involved in a more efficient ablation process in this time regime could be a Coulomb explosion if the electrons move beyond the NP border, leaving it highly charged. Further studies out of the scope of this paper are being carried out to clarify the mechanism of the ablation threshold for the picosecond regime.

If we compare the nonlinear absorption in each regime to the linear one at 532 nm, we can see that nonlinear absorption is negligible in both cases, and therefore no contribution to the ablation process is expected. However, as it has been indicated above, the saturation of the optical absorption is more relevant in the nanosecond regime than in the picosecond one. This result indicates that the sample becomes more transparent in the first case, absorbing less energy and therefore contributing to a higher ablation threshold. On the contrary, for the picosecond regime, this saturation being lesser important, the ablation threshold can be lower. It is notable that, contrary to intuition, due to this saturation of the optical absorption of the entire nanocomposite, which makes it more transparent, thermal effects characteristic of nanosecond pulses would not produce more damage to the sample than the picosecond ones.

IV. CONCLUSION

With a simple self-diffraction experiment, we reported saturable optical absorption and an important optical Kerr effect at 532 nm for pulses of 7 ns and 26 ps in a high-purity silica sample containing Cu NPs prepared by ion implantation. We showed the possibility for identifying the components of $\chi^{(3)}$ in an isotropic sample considering the vectorial self-diffraction effect for different mechanisms of nonlinearity of index, which are related to different components of $\chi^{(3)}$. We showed that thermal effect and induced polarization are the mechanisms responsible for the nonlinear response obtained for the nanosecond and the picosecond regimes, respectively. Our results indicate that the nanocomposite presents saturable absorption, which can be associated with the generation of hot electrons into the nanocomposite. It is worth remarking on the large differences between the nonlinear responses in both temporal regimes; we associated this result not only with the linear absorption of the incident light in the material but also with the different mechanisms present in each temporal regime. With respect to the ablation experiments, the ablation threshold was found to be lower for the picosecond regime and dependent on the spot area, in contrast to the nanosecond one, which is higher. While the principles of the mechanism for the ablation process in the

nanosecond regime are qualitatively well understood,[25,26] the physical process for the picosecond regime needs to be further studied.

ACKNOWLEDGMENTS

We acknowledge the partial financial support from DGAPA-UNAM through Grant Nos. IN108807-3, IN119706-3, and IN108407 and CONACyT-Mexico through Grant Nos. 42823-F and 50504.

[1]R. F. Haglund, Jr., L. Yang, R. H. Magruder III, J. E. Witting, K. Becker, and R. A. Zuhr, Opt. Lett. **18**, 373 (1993).
[2]J.-M. Lamarre, F. Billard, C. H. Kerboua, M. Lequime, S. Roorda, and L. Martinu, Opt. Commun. **281**, 331 (2008).
[3]A. L. Stepanov, C. Marques, E. Alves, R. C. da Silva, M. R. Silva, R. A. Ganeev, A. I. Ryasnyansky, and T. Usmanov, Tech. Phys. **51**, 1474 (2006).
[4]J. C. Cheang-Wong, A. Oliver, A. Crespo-Sosa, J. M. Hernández, E. Muñoz, and R. Espejel-Morales, Nucl. Instrum. Methods Phys. Res. B **161–163**, 1058 (2000).
[5]F. Gonella and P. Mazzoldi, *Handbook of Nanostructured Materials and Nanotechnology* (Academic, San Diego, 2000), Vol. 4, Chap. 2.
[6]R. W. Boyd, *Nonlinear Optics* (Academic, San Diego, 1992).
[7]M. Sheik-Bahae, A. A. Said, T. Wei, D. J. Hagan, and E. W. V. Stryland, IEEE J. Quantum Electron. **26**, 760 (1990).
[8]S. R. Friberg and P. W. Smith, IEEE J. Quantum Electron. **23**, 2089 (1987).
[9]C. Torres-Torres, A. V. Khomenko, J. C. Cheang-Wong, L. Rodríguez-Fernández, A. Crespo-Sosa, and A. Oliver, Opt. Express **15**, 9248 (2007).
[10]A. Oliver, J. C. Cheang-Wong, J. Roiz, L. Rodríguez-Fernández, J. M. Hernández, A. Crespo-Sosa, and E. Muñoz, Nucl. Instrum. Methods Phys. Res. B **191**, 333 (2002).
[11]O. Peña, J. C. Cheang-Wong, L. Rodríguez-Fernández, J. Arenas-Alatorre, A. Crespo-Sosa, V. Rodríguez-Iglesias, and A. Oliver, Nucl. Instrum. Methods Phys. Res. B **257**, 99 (2007).
[12]C. Torres-Torres and A. V. Khomenko, Rev. Mex de Física **51**, 162 (2005).
[13]T. E. Dutton, P. M. Rentzepis, T. P. Shen, J. Scholl, and D. Rogovin, J. Opt. Soc. Am. B **9**, 1843 (1992).
[14]F. Hache, D. Ricard, C. Flytzanis, and U. Kreibig, Appl. Phys. A: Mater. Sci. Process. **47**, 347 (2004).
[15]S. L. Logunov, T. S. Ahmadi, M. A. El-Sayed, J. T. Khoury, and R. L. Whetten, J. Phys. Chem. B **101**, 3713 (1988).
[16]P. V. Kamat, M. Flumiani, and G. V. Hartland, J. Phys. Chem. B **102**, 3123 (1998).
[17]B. Karthikeyan, M. Anija, C. S. Suchand Sandeep, T. M. Muhammad Nadeer, and R. Philip, Opt. Commun. **281**, 2933 (2008).
[18]R. Polloni, B. F. Scremin, P. Calvelli, E. Cataruzza, G. Battaglin, and G. Mattei, J. Non-Cryst. Solids **322**, 300 (2003).
[19]A. Ryasnyansky, B. Palpant, S. Debrus, R. I. Khaibullin, and A. L. Stepanov, J. Opt. Soc. Am. B **23**, 1348 (2006).
[20]J.-S. Kim, K.-S. Lee, and S. S. Kim, Thin Solid Films **515**, 2332 (2006).
[21]J. M. Ballesteros, R. Serna, J. Solís, C. N. Afonso, A. K. Petford-Long, D. H. Osborne, and R. F. Haglund, Jr., Appl. Phys. Lett. **71**, 2445 (1997).
[22]V. P. Drachev, A. K. Buin, H. Nakotte, and V. M. Shalaev, Nano Lett. **4**, 1535 (2004).
[23]A. Oliver, J. A. Reyes-Esqueda, J. C. Cheang-Wong, C. E. Román-Velázquez, A. Crespo-Sosa, L. Rodríguez-Fernández, J. A. Seman, and C. Noguez, Phys. Rev. B **74**, 245425 (2006).
[24]J. A. Reyes-Esqueda, C. Torres-Torres, J. C. Cheang-Wong, A. Crespo-Sosa, L. Rodríguez-Fernández, C. Noguez, and A. Oliver, Opt. Express **16**, 710 (2008).
[25]Z. Xia, J. Shao, Z. Fan, and S. Wu, Appl. Opt. **45**, 8253 (2006).
[26]A. Crespo-Sosa, P. Shaaf, J. A. Reyes-Esqueda, J. A. Seman-Harutinian, and A. Oliver, J. Phys. D **40**, 1890 (2007).
[27]I. M. Lifshits, M. I. Kaganov, and L. V. Taratanov, J. Nucl. Energy, Parts A/B **12**, 69 (1960); A. L. Stepanov, Rev. Adv. Mater. Sci. **4**, 123 (2003).